Yale University
EliScholar – A Digital Platform for Scholarly Publishing at Yale

Yale Medicine Thesis Digital Library | School of Medicine

9-21-2010

CFTR from divergent species respond differently to the channel inhibitors CFTRinh-172, glibenclamide, and GlyH-101

Marie Suzy Bewley
Yale University

Follow this and additional works at: http://elischolar.library.yale.edu/ymtdl

Recommended Citation
Bewley, Marie Suzy, "CFTR from divergent species respond differently to the channel inhibitors CFTRinh-172, glibenclamide, and GlyH-101" (2010). *Yale Medicine Thesis Digital Library*. 215.
http://elischolar.library.yale.edu/ymtdl/215

This Open Access Thesis is brought to you for free and open access by the School of Medicine at EliScholar – A Digital Platform for Scholarly Publishing at Yale. It has been accepted for inclusion in Yale Medicine Thesis Digital Library by an authorized administrator of EliScholar – A Digital Platform for Scholarly Publishing at Yale. For more information, please contact elischolar@yale.edu.

CFTR from divergent species respond differently to the channel inhibitors CFTRinh-172, glibenclamide, and GlyH-101

Marie S Bewley[1,2] Maximallian Stahl[1,2], Klaus Stahl[1,2], and John N. Forrest, Jr.[1,2]

[1]Nephrology Division, Department of Internal Medicine, Yale University School of Medicine, New Haven, New Haven, Connecticut, 06510

[2]The Mount Desert Island Biological Laboratory, Salisbury Cove, Maine, 0467

YALE SCHOOL OF MEDICINE THESIS 2010

Student: Marie Bewley

Faculty Advisor: John Nevins Forrest Jr., MD

Abstract

Studies of widely diverse species of a protein are a powerful tool to gain information on the structure and function of the protein. We investigated the response of human, pig, shark and killifish cystic fibrosis trans-membrane conductance regulator (CFTR) to specific inhibitors of the channel: CFTRinh-172, GlyH-101, and glibenclamide. In several expression systems, including isolated perfusions of the rectal gland, primary cell cultures of rectal gland tubules and oocyte expression, we observed fundamental differences in the sensitivity to inhibition by these CFTR blockers. We used primarily two-electrode voltage clamping of cRNA microinjected *Xenopus laevis* oocytes. In oocyte studies, shark CFTR was insensitive to CFTRinh-172 (maximum inhibition 8 ± 1.4% at 20μM), pCFTR was insensitive to Glibenclamide (maximum inhibition 12.8 ± 4.2% at 200μM), and all species were sensitive to GlyH-101 (maximum inhibition with pCFTR of 80.2 ± 3.6% at 20μM). Shark CFTR was completely insensitive to inhibition by CFTRinh-172 in short circuit current experiments (2.5 ± 0.15 % inhibition of chloride secretion) compared to inhibition with GlyH-101 (56.5 ± 6.56 % inhibition of chloride secretion). Perfusion studies confirmed these results. These experiments demonstrate a profound difference in the sensitivity of different CFTR species to inhibition by CFTR blockers. However, the amino acid residues that have been proposed by site directed mutagenesis studies to be responsible for inhibitor binding are uniformly conserved in all four isoforms studied. Therefore, the differences cannot be explained by simply targeting one amino acid for site-directed mutagenesis. Rather, the potency of the inhibitory actions of CFTRinh-172, Gly-H101 and glibenclamide on the CFTR molecule is dictated by the local environment and the three dimensional structure of residues that form the vestibule and the chloride pore.

Aknowledgements: I would above all like to thank Max and Klaus Stahl for their overwhelming kindness and help in carrying out pig and killifish CFTR oocyte experiments and for their work with human and shark CFTR full inhibitor experiments and for their immense experimental and written contributions to this project. I would also like to thank on behalf of Max and Klaus, Denry Sato, Christine Chaplin and Catherine Kelley for their help. Thank you to my thesis advisor, Dr. John Forrest and to my thesis reader, Dr. Emile Boulpaep.

Table of Contents

Introduction

Overview of Cystic Fibrosis

Cystic fibrosis (CF) is a prototypical example of a simple mutation in a single gene that ultimately causes a complex disease. (1-2) CF is caused by mutations in the cystic fibrosis trans-membrane conductance regulator (CFTR) protein, a chloride channel and regulatory protein found in exocrine glandular tissues. As a result, CF is a disorder of exocrine function involving multiple organ systems. The autosomal recessive disorder is the most common lethal inherited disease in the Caucasian population and affects more than 1 in 3000 live births. (3) The current median age of survival is 36.9 years of age, with affected males typically living longer than affected females. (3) Diagnosis of CF is made by evidence of clinical manifestations of CF in at least one organ system and evidence of abnormal chloride secretion: an elevated sweat chloride (>60 mmol/L) on two occasions, presence of two disease causing mutations or an abnormal nasal potential difference. While there are over 1,400 mutations in the CFTR gene reported to cause CF, the most common mutation, ΔF508 is a deletion of the three nucleotides encoding phenylalanine at position 508. This mutation accounts for over two thirds of CF cases worldwide and 90% of the cases in the United States. (4)

CF is caused by defective CFTR mediated chloride transport which causes increased sodium and water absorption across epithelial cells and results in thick viscous secretions in the pancreas, lung, liver, intestine, reproductive tract and dermis. (5) Clinical manifestations of CF are recurrent respiratory infections, pancreatic enzyme insufficiency, and elevated sweat chloride levels. Respiratory manifestations occur in nearly 90% of homozygous patients who survive infancy. Increased airways secretions caused by defective chloride secretion causes decreased muco-cilliary function and defective clearance of the airways. As a result, CF patients become colonized at an early age with pathogenic bacteria, often *Staphylococcus aureus* and *Pseudomonas aeruginosa*. Patients develop a persistent chronic cough, hyperinflation of the lungs, and pulmonary function tests demonstrate obstructive airway disease. As the disease progresses, chronic bronchitis is accompanied by malaise, anorexia, weight loss and digital clubbing. Typically, CF patients ultimately succumb to complications related to their pulmonary disease. (5-6)

Due to the multi-system clinical manifestations of the disease, treatment regimes for CF patients typically involve a team of specialists including pulmonary, endocrine and nutritional specialists. The primary goal of CF treatment includes maintaining lung function, controlling respiratory infections,

clearing mucus from the airways and administering nutritional therapy to offset pancreatic insufficiency. Acute pulmonary exacerbations are often treated at home but frequently require hospitalization. Current therapies include, chest physical therapy, postural drainage, inhaled bronchodilator treatment, administration of Dornase alfa and inhaled and intravenous antibiotics. (6-7) Gene therapy, correction of abnormal protein folding, improvement of endogenous ion channel function and induction of alternate channels are some of novel therapeutic strategies for CF that are being explored with variable success in clinical trials. (6-7)

Cystic Fibrosis Transmembrane Conductance Regulator

CFTR is a phosphorylation dependent epithelial chloride channel located in the apical membrane of epithelial cells in the lungs, liver, pancreas, digestive tract, reproductive tract and skin. (5-9) The identification of the primary sequence of CFTR was made in 1989 and CFTR was classified as a part of the ATP binding cassette (ABC) transporters, traffic ATPases that use the energy from ATP hydrolysis for transport. (13-14) The complete structure of the CFTR protein has not yet been experimentally determined by X-ray crystallography largely because the significantly hydrophobic trans-membrane regions are difficult to crystallize. Currently only low-resolution structures of the several domains of the protein

exist (15). CFTR contains five domains, membrane spanning domains (MSD1 and MSD2) each with six trans-membrane helices, two nucleotide-binding domains (NBD1 and NBD2), and one regulatory domain (R). The two membrane spanning domains are separated and connected by the NBDs and the R domain. The transport of ions is thought to be driven by ATP binding and hydrolysis at the NBDs which causes dimerization of the NBDs and opening of the channel forming helices (6). Regulation of CFTR mediated chloride transport occurs by modification of the R domain through cyclic-AMP dependent addition or removal of phosphate groups. (1, 11) (Figure 1)

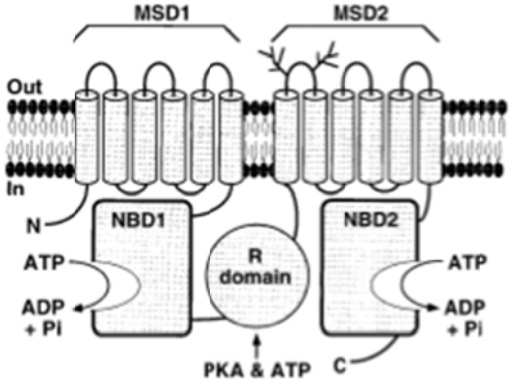

Figure 1: Model showing the proposed domain structure of CFTR. MSD, membrane-spanning domain; NBD, nucleotide-binding domain; R, regulatory domain; PKA, cAMP-dependent protein kinase. (1)

CFTR mediated Ion Permeation

CFTR is one of the only ABC transporters known to be an ion channel. Thus, the study of CFTR's channel function provides a unique glimpse of the ABC transporter mechanism.

Ion permeation is influenced by the presence of charged amino acid side chains at the entrance of the channel pore (16). These specific residues attract oppositely charged ions, which increase the effective local concentration, while also repelling ions of similar charge. Site directed mutagenesis studies have been used to identify the role of positive charged residues in ion conductance (17-18). Functional evidence suggests that permeant anions bind to several discrete sites within the CFTR channel pore (19-24). These binding sites may be involved in attracting chloride ions into the CFTR pore (21) and in coordinating ion-ion interactions that are necessary for rapid ion movement through the pore (24-26).

Specific inhibitors of the CFTR channel have been employed as tools to investigate further the role of key amino acids in the channel pore. Chloride ion binding sites within the pore may also be binding sites for small molecules that occlude the pore and thus inhibit chloride transport. (25, 30-31) Several organic anions have been demonstrated to occlude and inhibit chloride transport, including glibenclamide, a sulfonourea (31, 34-35), CFTRinh-172 a thiazolidone (36-39), and GlyH-101, a glycine hydrazide (40). Glibenclamide and GlyH-101 are thought to act as open channel blockers: glibenclamide acting from the internal membrane surface and GlyH-101 from the external surface. CFTRinh-172 is thought to bind at the R domain and does not act as an open channel

blocker. (37) Initial studies suggest that CFTRinh-172 acts optimally during the open state of the channel. (36-39) However, despite numerous site-specific mutagenesis studies, the location and number of those inhibitor binding sides remain unclear (30, 43-46).

An important limitation of site directed mutagenesis studies is that manipulation of the amino acid sequence may cause disruption of important secondary or tertiary structural relationships thus causing inaccurate conclusions regarding changes in protein function observed or relative importance of mutated amino acids. Cross species comparison studies serve as a powerful method to analyze structure and function relationships (41-42, 47-48). The evolutionary differences in amino acid sequences that arise over time and the conservation of specific motifs in different species help to define the functional significance of specific amino acids without the limitations of site directed mutagenesis.

Statement of Purpose

Several years ago, members of our lab observed profound differences in the response of shark and human CFTR in response to three thiol-reactive substances: mercury, zinc and glutathione. Site-specific mutations introduced at shark unique cysteines in human CFTR revealed restoration of sensitivity to

mercury mediated inhibition only observed in shark. (41-42) At this time, our lab also observed that the novel CFTR specific inhibitor, CFTRinh-172, did not inhibit CFTR mediated chloride secretion in short circuit current studies of shark rectal gland tissues monolayers and in perfusion studies of the intact shark rectal gland. These preliminary experiments prompted me, several years ago, to explore the apparent species differences between shark and human CFTR in response to CFTRinh-172 using two-electrode voltage clamping of *Xenopus laevis* oocytes. I discovered that shark indeed was not sensitive to the significant inhibition of conductance seen in the human ortholog of CFTR**.** (49) Realizing that CFTRinh-172, glibenclamide and GlyH-101 may all inhibit chloride permeation through interactions with the pore, my work has been expanded to study the inhibition of all three CFTR specific inhibitors on four species of CFTR: shark, human, pig and killifish. The purpose of this work was to explore the pharmacologic profiles of these CFTR specific inhibitors across several species to elaborate structural and functional relationships.

Materials and Methods

This student participated in the shark rectal gland perfusion studies, the measurement of short circuit current, the synthesis of human and shark CFTR cRNA, the harvesting and injection of X*enopus laevis* oocytes, and initial studies

of CFTR specific inhibitor, CFTRinh-172, on shark and human CFTR. Other colleagues in the lab, specifically Klaus and Max Stahl carried out additional studies in pig and killifish CFTR with the multiple inhibitors.

In vitro perfusion of shark rectal glands.

Rectal glands were obtained from either sex of dogfish sharks, *Squalus acanthias*, weighing 2-6 kg. Glands were removed and cannulae were placed in the single artery, vein and duct as described previously (33). Glands were placed in a glass perfusion chamber at 15°C equilibrated with running seawater. Glands were perfused with an elasmobranch Ringer's solution (270mM NaCl, 4mM KCl, 3mM MgCI2, 2.5 mM CaCi2, 1 mM KH2PO4, 8mM NaHCO3, 350mM urea, 5mM glucose, and 0.5 mM Na2SO4) (all from Sigma Chemical Co., St. Louis, MO) and equilibrated to pH 7.5 by bubbling with 99% 02 and 1% CO2. The glands were perfused with shark Ringers solution for thirty minutes to reach basal levels of chloride secretion (~250μEq/h/g). Forskolin and IBMX were added to the solution at 1μM and 100μM respectively. Chloride secretion was measured in 1-min intervals. After twenty minutes of stimulated secretion, 10μM CFTRinh-172 was added to the perfusion solution for thirty additional minutes (50-80min) and then removed. Measurements of duct flow were made at 10-min intervals in

all experiments. Results are expressed as micro equivalents of chloride secreted per hour per gram wet weight (μEq/h/g)p ±SEM.

Primary Cell Cultures of Shark Rectal Gland Tubules.

Primary cultures of shark rectal gland epithelial cell monolayers were prepared per a protocol previously described (43). Rectal glands were excised under sterile conditions, sliced horizontally into 2-3 mm sections, and minced into a slurry with two sterile scalpel blades. The mince was transferred into a 50 ml conical tube and washed 3x with 20 ml of sterile shark Ringer's. The mince was suspended in a collagenase solution (0.2% in 30 ml of sterile shark Ringer's) and incubated at 25˚C for 1 hour under constant agitation. At the end of the incubation, the suspension was washed with sterile shark Ringer's by centrifugation at 200xg at 4˚C for 45 seconds. The supernatant was discarded and the pellet was re-suspended in 20 ml of sterile shark Ringer's. The digested mince was agitated to release the tubules into the supernatant. The suspended tubules were harvested and kept on ice. Suspension, agitation, and harvesting of the tubules were repeated two more times. The tubules were next washed and suspended in 20 ml of sterile shark Ringer's, from which two 1 ml aliquots were removed to determine the total yield by wet weight. Average yields were 250-500 mg wet wt/gland. The tubules were then suspended in a medium composed of

Dulbecco's Modified Eagle's Medium/Ham's F-12 (15 mM HEPES, 3.9 mM $CaCl_2$, 2.5 mM $MgCl_2$, 300 mM urea, 94 mM NaCl, 150 mM trimethylamine oxide, 21 mM $NaHCO_3$, 10 ml/l penicillin/streptomycin (10000 U x 10 mg^{-1} x ml^{-1}), 10 ml/l ITS^+, and 50 ml/l Nu-Serum). Tubules, at a density of ~10 mg/ml, were seeded onto 1.2 ml rat tail collagen gels (Cohesion Technologies) in 35 mm dishes supported with 150 µm nylon mesh. The tubules were allowed to grow to confluence at 18°C under 95% O_2 and 5% CO_2, typically within 10-14 days. The nylon mesh containing the monolayer of cells was excised from the petri dish using a sterile scalpel blade and mounted in an Ussing chamber. Both the apical and basolateral sides of the monolayer were bathed with shark Ringer's containing 5 mM glucose at pH 7.5.

Measurements of Transepithelial Chloride Transport as Short Circuit Current (I_{sc}) in Primary Culture Monolayers: inhibition with CFTRinh-172 and GlyH101

Confluent cultures were mounted in a conventional Plexiglas® Ussing chamber with an aperture of 0.28 cm^2. Both hemi-chambers were independently perfused by gravity flow at room temp (20-22˚C) with shark Ringer's solution and 95% O_2 - 5% CO_2. Trans-epithelial voltages were measured with an Iowa dual voltage clamp (model 710C) and agar bridges connected to calomel electrodes

using methods previously described (43-44). The bridges were filled with shark Ringer solution and were positioned approximately 1 mm from the apical and basolateral surfaces of culture. Trans-epithelial resistance was measured by applying bipolar current pulses every 50 seconds. The voltage clamp administered current via agar bridges linked to external Ag-AgCl electrodes. Short circuit current (I_{sc}), or net electrogenic chloride secretion (43), was measured by determining the current necessary to clamp the spontaneous trans-epithelial voltage to 0 mV. Inhibition by CFTRinh-172 and GlyH101 was determined by the ratio of Isc measured at the peak of stimulation (1μM Forskolin) and Isc at the highest concentration of the inhibitors. Results are expressed as microampere per cm^2 ($\mu A/cm^2$) ± SE.

To study GlyH-101, the organic compound was added after steady state conditions were reached at concentrations of 30, 60, 90 and 120μM to the mucosal side of the monolayers. The study of CFTRinh-172 was similar to that of GlyH-101.

Synthesis of hCFTR, pCFTR, kfCFTR, and sCFTR cRNA:

All CFTR orthologues were cloned into T7 expression vectors. Human, shark and pig CFTR sequences were in pcDNA3.1, whereas kfCFTR was in pGEMTeasy expression vector. The vectors were grown up in 150ml cultures of

TOP10 electrically competent E. coli (Invitrogen, Crlsbad, CA) and subsequently isolated using Pure Yield Maxiprep Systems (Promega, Madison, Wisconsin). The clones were whole length sequenced to confirm the integrity of the CFTR ORFs. 12μg CFTR DNA was linearized with XhoI and purified by PCR purification (Qiagen, Alameda, CA). Capped cDNA was synthesized using T7 RNA polymerase and in vitro transcription following the instructions of T7 in vitro transcription system (Ambion, Austin, TX). The reaction products were precipitated using lithium-chloride precipitation and tested with the Agilent Bioanalyzer system (Agilent, Santa Clara, CA). (50)

Oocyte preparation and expression of hCFTR, pCFTR, kfCFTR and sCFTR.

Mature female *Xenopus laevis* (Xenopus I, Dexter, Michigan) were anesthesized in a 0.15 % cold solution of tricaine for 20min, and several ovarian lobules were removed under sterile conditions through an abdominal incision per the protocol approved by the Yale University Institutional Animal Care and Use Committee. The ovarian lobules were manually dissected in smaller pieces and kept in calcium free ND96 (96mM NaCl, 1mM KCl, 1mM MgCI2·6H2O, 5mM HEPES (1/2 Na) equilibrated to pH 7.5) (all from Sigma Chemical Co., St. Louis, MO). Oocytes were de-folliculated by incubating in a 2.5mg/ml solution of type I collagenase for 2 hours and subsequently treating with a hypertonic potassium

phosphate solution. Mature stage V and VI oocytes were selected and stored in modified Barth solution (MBS) (88mM NaCl, 1mM KCl, 2.4mM NaHCO3, 0.82mM MgSO4·7H2O, 0.33mM Ca(NO3)·4H2O, 0.41mM CaCl2·H2O, 10mM HEPES (1/2 Na) and 1% Penicillin/Streptomycin equilibrated to pH 7.4) (all from Sigma Chemical Co., St. Louis, MO) at 18°C. The oocytes were injected with 1-5ng of cRNA / 50nl or an equivalent volume of water and stored for 1-2 days in MBS at 18°C. (50)

Two electrode voltage clamping: inhibition of hCFTR, pCFTR, kfCFTR and sCFTR with CFTRinh-172, GlyH101, and Glibenclamide.

Electrophysiological recordings were performed 1-2 days after injection of the cRNA. Electrodes were pulled on a micropipette puller (Sutter Instruments, Novata, CA), the electrodes were filled with 3M KCl and had input resistances between 0.6 and 1.3 MΩ. During two-electrode voltage clamping recording, current-voltage (I-V) curves were obtained by clamping the voltage over a ramp from -120 to +60 mV at a rate of 100mv/s with the use of a two-electrode voltage clamp (TEV-200, Dagan Instruments, Foster City, CA). After correcting for capacity currents, reversal potentials were determined and conductances were calculated over a range of ±20mV. During the experiment, the oocytes were perfused with calcium containing ND96 (ND96 in addition of 1.8mM CaCl2·H2O). I-V ramps were taken under basal conditions and during stimulation

by forskolin (10μM) and IBMX (1mM). Once the stimulation reached a steady state, the different inhibitors were added beginning with the smallest inhibitor concentration. Once currents with one concentration of the specific inhibitor reached a steady state, the next higher concentration of the same inhibitor was used. IBMX and Forskolin were used continuously throughout stimulation and inhibition. Washout was performed with ND96 alone. The inhibitors used were $CFTR_{inh}$-172 (Sigma, Cystic fibrosis therapeuticals), GlyH-101 (Cystic fibrosis therapeuticals) and Glibenclamide (Sigma) at concentrations of 5, 10 and 20 μM. The maximum dose of 20μM was used for two reasons: first at greater concentrations of drug used, solubility became a factor and secondly, 20 μM was near maximum inhibition demonstrated in all species. In all experiments inhibition was determined by the ratio of the conductance measured at steady state conductance of IBMX and Forskolin mediated stimulation and the conductance obtained at the steady state of inhibition by the specific dose of the specific inhibitor. Data was analyzed with pCLAMP software. Results are expressed as micro Siemens (μS) ± SE.

Results

Measurements of Trans-epithelial Chloride Transport as Short Circuit Current (I_{sc}) in Primary Culture Monolayers: Inhibition with CFTRinh-172 and GlyH101

GlyH-101: Chloride secretion.

GlyH-101 significantly inhibits sCFTR-mediated secretion of short circuit current (41.3 ± 3.0 % inhibition). Individual experiments (results not shown here) demonstrate that the addition of 10μM CNP, 20μM milrinone and 10μM forskolin cause the Isc to increase and reach steady state activation after 50 minutes with a steady state current of about 50 μA. After the addition of GlyH-101 (30, 60, 90 and 120μM) the current decreases in a dose specific step-wise fashion to currents below 30μA. (Figure 8)

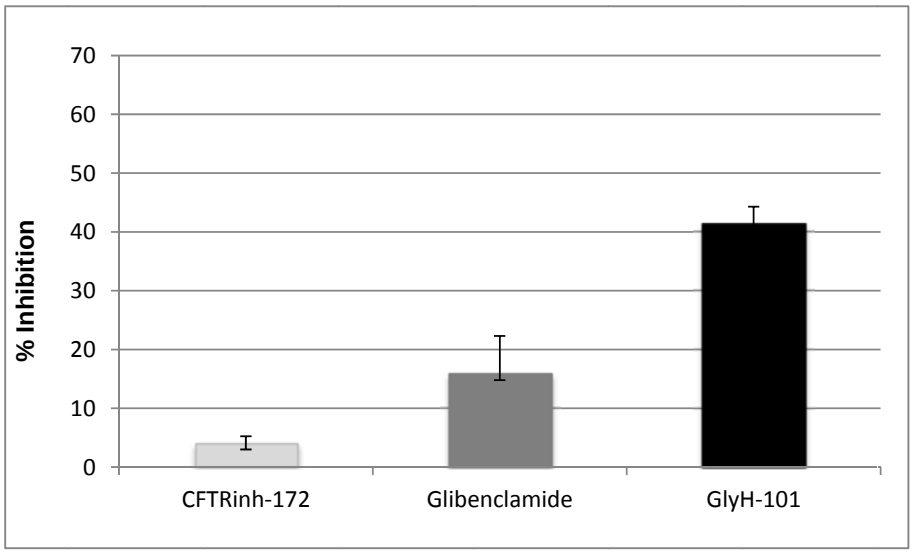

Figure 2: In primary cultured SRG epithelial cells, chloride transport, measured as Isc was first stimulated by secretagogues (forskolin 10 μM and IBMX 100 μM) and Isc increased from base line values of 9.4 ± 5.7 μA/Cm^2 to 69 ± 16.5 μA/Cm^2 to inhibitors (CFTRinh-172,

glibenclamide, and GlyH-101 were then added and the mean % inhibition was calculated (n=4-6 per group).

Glibenclamide: Chloride secretion

Individual experiments demonstrate a modest inhibition of chloride secretion by glibenclamide when compated to gly-H inhibition. (15.8 +/- 16.5 % inhibition of Isc)

CFTRinh-172: Chloride secretion.

Individual experiments demonstrate activation of Isc from basal values after the addition of 10μM Forskolin and 1μM VIP. Steady state stimulation occurs after 40 min with Isc currents typically greater than 80 μA. The addition of GlyH-101 to this activating cocktail again causes a similar decrease in current to values below 60μA as was demonstrated in the previously described experiments. However, the addition of 50μM CFTRinh-172 to the perfusate does not cause a further decrease in short circuit current but rather the current is observed to remain at the steady state currents observed after the addition of GlyH-101. Figure 2 demonstrates the percent inhibition in shark CFTR mediated chloride secretion by GlyH-101 (n=4) and CFTRinh-172 (n=3). CFTRinh-172, in contrast to GlyH-101, does not inhibit sCFTR secretion short

circuit current (CFTRinh-172; 2.5 ± 0.15 % inhibition, GlyH-101; 56.5 ± 6.55749 % inhibition).

Conductance of hCFTR, kfCFTR, pCFTR, sCFTR and un-injected and water injected controls under basal and stimulated conditions.

The conductance of oocytes was measured 2-3 days post injection in 109 oocytes injected with hCFTR (n=20), kfCFTR (n=25), pCFTR (n=21), sCFTR (n=15), water (n=12) and un-injected (n=12). Human CFTR, kfCFTR, pCFTR and sCFTR had basal conductances of 11.9 ± 1.4 μS, 20.5 ± 1.9 μS, 13 ± 3.3 μS and 6.7 ± 1.3 μS respectively. Un-injected and water injected control oocytes had a significantly lower baseline conductance of 7.2 ± 1.2 μS and 6.2 ± 0.6 μS, respectively ($P < 0.05$) compared with baseline conductances of hCFTR, kfCFTR, pCFTR and sCFTR.

Because the aim of the study was to study the effects of CFTR specific inhibitors after activation of CFTR, it was important to establish comparable steady state conductances amongst the four species of CFTR. After the addition of 10μM forskolin and 1mM IBMX to the perfusate, hCFTR, kfCFTR, pCFTR and sCFTR had similar steady state conductances (206 ± 21.9 μS, 218.7 ± 14.3, 160.1 ± 29.5 μS and 160.7 ± 34 μS). While the steady state activated conductances of hCFTR and kfCFTR appeared larger than those of pCFTR and

sCFTR, these observed differences were not statistically significant and likely were secondary to natural differences in oocyte batches and differences due to daily conductance variability. In the control un-injected and water injected oocytes, the conductance after stimulation with IBMX and forskolin remained similar to the conductances measured at baseline (5.9 ± 1.6 μS and 5.8 ± 0.5 μS). The basal and stimulated conductances in control oocytes were significantly lower than those of all species of CFTR under both basal and steady state stimulated conditions ($P < 0.001$). (Figure 3)

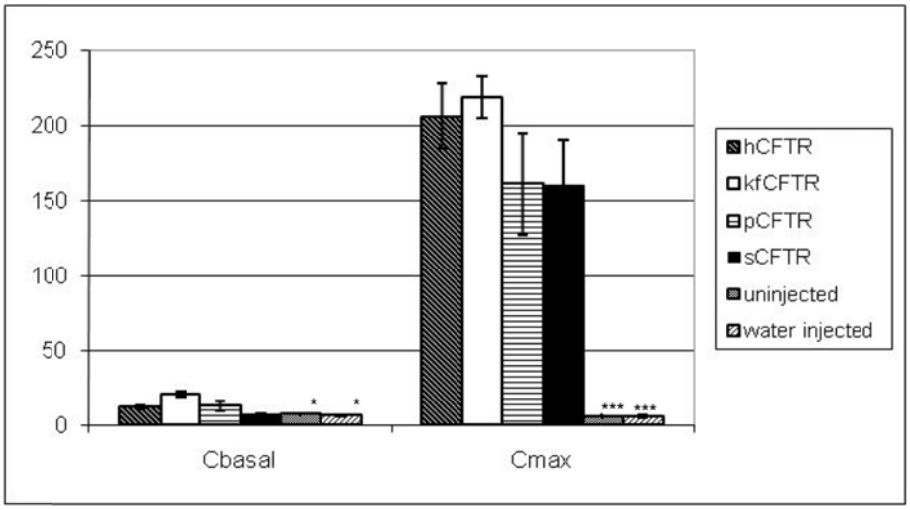

Figure 3: Conductances of Xenopus oocytes expressing hCFTR (n=20), kfCFTR (n=25), pCFTR (n=21), sCFTR (n=15) and uninjected (n=12) or water injected (n=12) oocytes as negative controls. Un-injected and water injected control oocytes had a significant lower baseline conductance and a highly significant lower steady state conductance than hCFTR ($P < 0.05$ and < 0.001, respectively). The baseline and steady state conductances of the four species did not differ significantly. Conductance is measured on the

Comparison of CFTR specific inhibitors, CFTRinh-172, GlyH101 and Glibenclamide across species of CFTR mediated conductance.

The conductance changes over time are demonstrated in representative experiments in Figure 4. In all species of CFTR, stimulation with forskolin and IBMX resulted in a prompt increase in conductance, which reached a steady state after 20-30 minutes. The addition of inhibitors to the perfusate consequently caused a decrease in conductance. The dose response of the CFTR mediated conductance is observed as a stepwise decrease in conductance as increasing concentrations of the specific inhibitors are added to the perfusate. In contrast to the similarities observed across species of CFTR after stimulation by forskolin and IBMX, the response to each inhibitor was different across species.

The I-V relationships for the oocytes are demonstrated in Figures 5b and 6b. Throughout all experiments, all species of CFTR injected oocytes exhibited similar linear I-V relationships. After the addition of forskolin and IBMX, the reversal potentials depolarized toward the resting potential of chloride. Similarly, after the addition of the various inhibitors that caused inhibition of CFTR mediated anion conductance, the reversal potential re-polarized toward basal values.

CFTRinh-172: sCFTR is unresponsive to CFTRinh-172

A dose response comparison was made across species of CFTR with 5, 10, and 20μM of CFTRinh-172. CFTRinh-172 inhibited hCFTR significantly (15.9 ± 2.9% inhibition at 5μM, 39.8 ± 3.7% at 10μM and 61.2 ± 3.2% at 20μM). However, a less prominent response to CFTRinh-172 was observed in kfCFTR and pCFTR, particularly at higher doses (43.5 ± 5% and 20.6 ± 5.1% inhibition at 20μM, respectively) (Figure 5A)

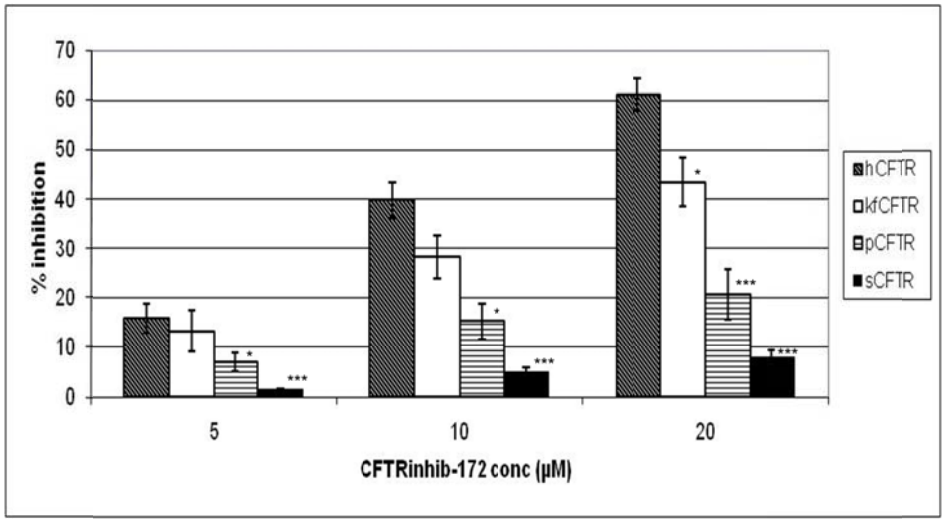

Figure 5*: Comparison of the effects of CFTRin-172 on CFTR species.*

A: Summary of % Inhibition of h-, kf-, p- and sCFTR with 5, 10 and 20 μM of CFTRinh-172. sCFTR was almost unresponsive to CFTRinhib172 (1.5 ± 0.2% inhibition at 5μM, 5 ± 0.8% at 10μM, 8 ± 1.4% at 20μM). The absence of inhibition of sCFTR by CFTRinh-172 is highly significantly (P=0.001 for 5μM, P=1.5x10-5 for 10μM and P=2x10-7 for 20μM) compared to hCFTR.

Interestingly, sCFTR was almost completely unresponsive to CFTRinh-172 (1.5 ± 0.2% inhibition at 5μM, 5 ± 0.8% at 10μM, 8 ± 1.4% at 20μM). The inhibition of

sCFTR by CFTRinh-172 is highly significant (P=0.001 for 5µM, P=1.5*10-5for 10µM and P=2*10-7 for 20µM) when compared to hCFTR. (Figure 5a)

I-V plots for both species are shown in Figure 5b and demonstrate similar currents between between human and sCFTR at basal and stimulated conditions and different responses in current after addition of CFTRinh-172 to the perfusate. I-V ramps were taken at the end of each of the following conditions: baseline perfusion with frog ringer solution until the conductance reached a baseline steady state, stimulation with forskolin (10µM) and IBMX (1mM) until conductance reached a new steady state and inhibition with CFTRinh-172 (20µM).

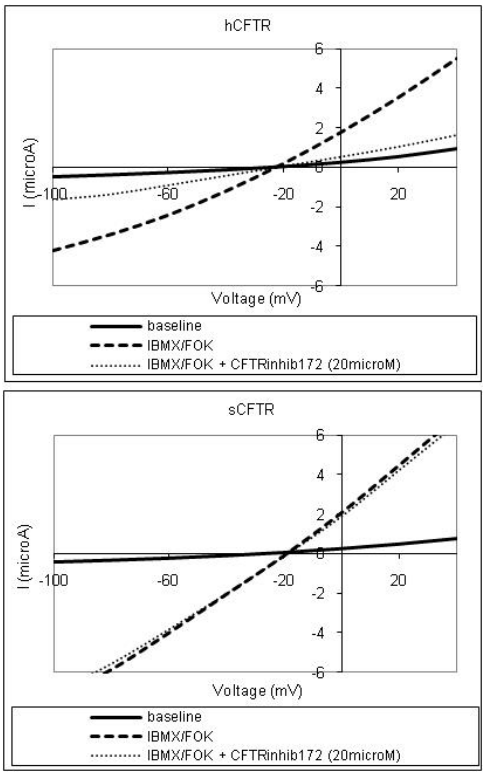

Figure 5: *Comparison of the effects of CFTRin-172 on CFTR species.*

B: Representative I-V plots from oocytes expressing h- and sCFTR. Human- and sCFTR show similar currents at baseline and after stimulation. However, they differ significantly in the currents they exhibit after inhibition with CFTRinhib172.

To further explore the findings that sCFTR is unresponsive to CFTRinh-172, *in vitro* inhibition was examined using both isolated shark rectal glands in perfusion studies and by measurement of short circuit current (I_{sc}) in primary culture monolayers of rectal gland tubular cells. Perfusion studies confirmed that

$CFTR_{inh}$–172 had no effect on chloride secretion in the shark rectal gland (Figure 6). The effects of $CFTR_{inh}$–172 on chloride secretion in rectal gland monolayer cells were consistent with the perfusion studies. Addition of 1, 5 and 10 μM $CFTR_{inh}$–172 to 1 μM forskolin and 100 μM IBMX stimulated cells showed no inhibition in four experiments (results not shown).

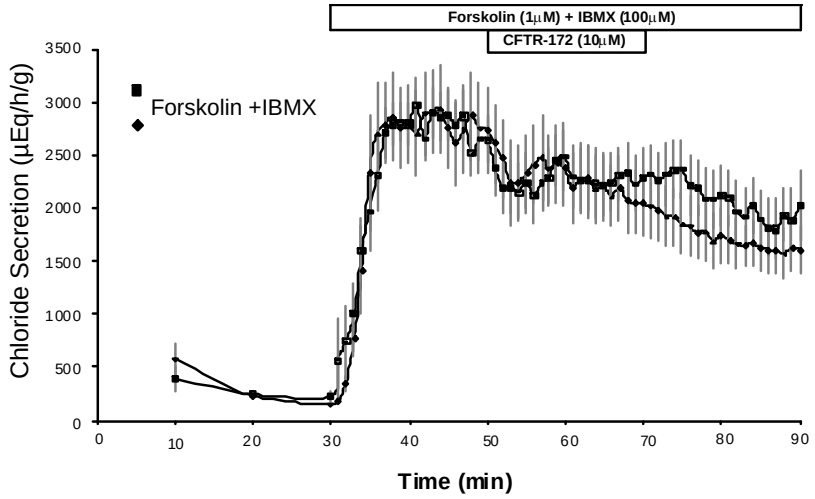

Figure 6: Chloride secretion in perfused shark rectal glands with 1 μM forskolin and 100 μM IBMX added to the perfusate. CFTRinh–172 (10 μM) was added from 50-70 min in experimental studies (n=5) and effects were compared to controls (n=18). Values are mean ± SEM. Forskolin and IBMX are squares, CFTRinh-172 are diamonds.

Glibenclamide: pCFTR is unresponsive to Glibenclamide

Similar to the experiments with CFTRinh-172, we compared the dose response of the four different CFTR species to glibenclamide (5, 10 and 20μM). Glibenclamide inhibited hCFTR significantly (29.7 ± 3.7% inhibition at 5μM, 44.6 ± 1.9% at 10 μM and 61.3 ± 3.7% at 20μM). Unlike CFTRinh-172, sCFTR was

responsive to glibenclamide (30.2 ± 4.5% inhibition at 5µM, 40 ± 8.6% at 10 µM and 52.2 ± 7.7% at 20µM) (Figure 7a). Similar to CFTRinh-172, kfCFTR was also less.

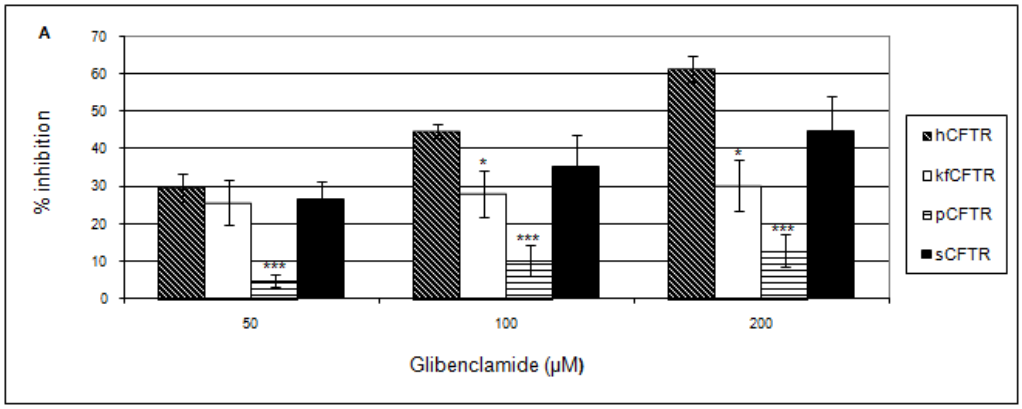

Figure 7*: Comparison of the effects of Gibenclamide on CFTR species.*

A: Summary of % Inhibition of h-, kf-, p- and sCFTR with 50, 100 and 200 µM of Glibenclamide. Importantly, % inhibition of pCFTR by Glibenclamide (4.9 ± 1.7% inhibition at 5µM, 10.2 ± 4.2% at 10 µM and 12.8 ± 4.2% at 20µM) was highly significant at all concentrations studied ($p<0.001$) when compared to human.

Interestingly, pCFTR was highly significantly unresponsive to glibenclamide (4.9 ± 1.7% inhibition at 5µM, 10.2 ± 4.2% at 10 µM and 12.8 ± 4.2% at 20µM, $P < 0.001$ in all concentrations) in comparison to human.

I-V plots for both species are shown in Figure 7b and demonstrate similar currents between human and pCFTR at basal and stimulated conditions and different responses in current after addition of glibenclamide to the perfusate.

These results are supported by recently reported observations in short circuit current studies with human, pig, ferret and mouse that pCFTR is less sensitive than hCFTR to glibenclamide (48).

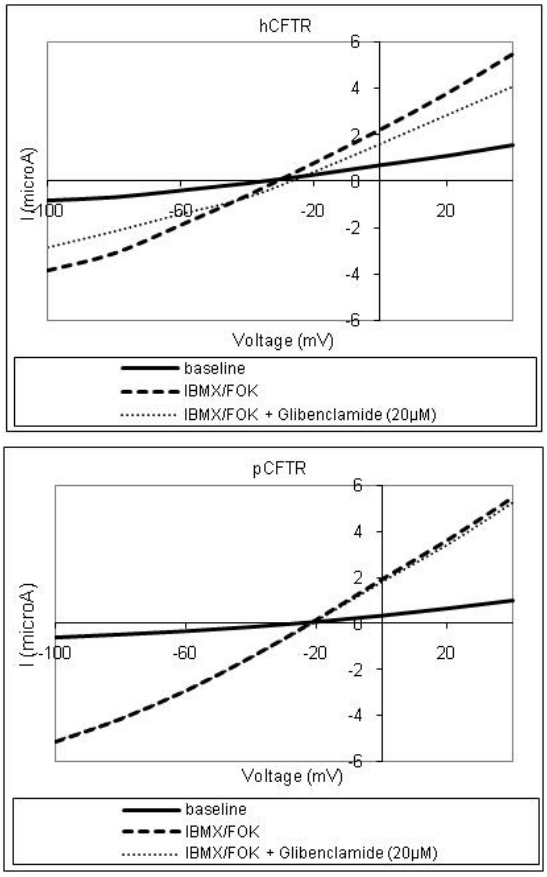

Figure 7: *Comparison of the effects of Glibenclamide on different CFTR species.*

B: Representative I-V plots from oocytes expressing h- and pCFTR. Human- and pCFTR show similar currents at baseline and after stimulation. However, they differ significantly in the currents they exhibit after inhibition with Glibenclamide.

GlyH-101: All species are responsive to GlyH-101

In contrast to CFTRinh-172 and glibenclamide, hCFTR, kfCFTR, sCFTR and pCFTR are all responsive to GlyH-101. This inhibition is particularly evident at the highest concentration used (20µM). Shark, kfCFTR and pCFTR are inhibited more by GlyH-101 than hCFTR (hCFTR: 47.8 ± 4.7%; kfCFTR: 58.1 ±

3.9 %; pCFTR: 80.2 ± 3.6%; sCFTR: 70.1 ± 3.8 %). Shark and pig's sensitivity was highly significant at 20μM ($P < 0.001$). Additionally, sCFTR shows a prompt response to GlyH-101 inhibition at the lowest concentration of GlyH-101 studied (49.3 ± 3.3 % in contrast to 20.2 ± 3.8 % with hCFTR). (Figure 8)

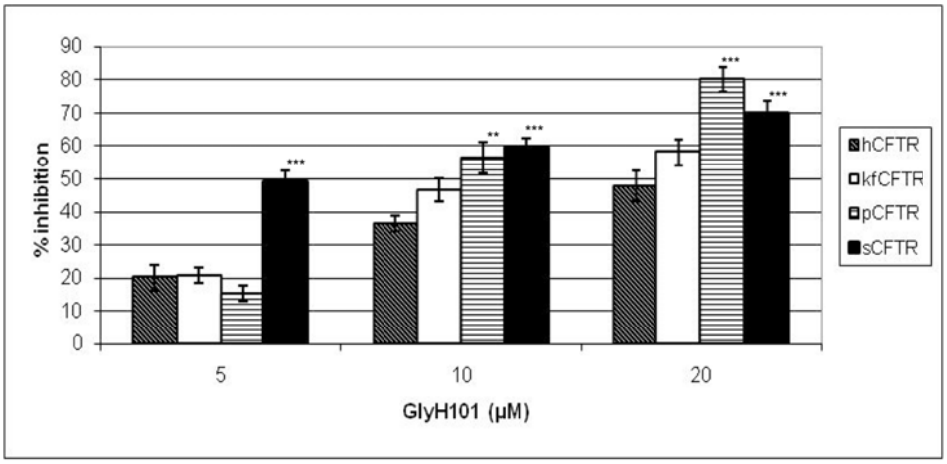

Figure 8: *Comparison of the effects of GlyH-101 on different CFTR species.*
Summary of % Inhibition of h-, kf-, p- and sCFTR with 5, 10 and 20 μM of GlyH-101. All species are responsive to GlyH-101. At 20μM, kfCFTR, sCFTR and pCFTR are significantly more inhibited by GlyH-101 than the human isoform (hCFTR: 47.8 ± 4.7%; kfCFTR: 58.1 ± 3.9 %; pCFTR: 80.2 ± 3.6%; sCFTR: 70.1 ± 3.8 %). Shark CFTR is highly significantly more sensitive ($P < 0.001$) to GlyH-101mediated inhibition of chloride current than hCFTR at all concentrations studied and pCFTR is highly significant at 20μM ($P < 0.001$).

Discussion

Reverse Pharmacology of CFTR

The "reverse pharmacology" method of analyzing the relationship between structure and function of ion channels is dependent on the use of pharmacologic

agents that are known to interact with and block the ion channel. (58) These small molecule pore blocking agents are used as probes of the ion pore to analyze the effects of mutagenesis on blocking behavior. The term "reverse pharmacology" was coined because the known structure of the inhibitor was used to investigate the unknown contours of the channel pore. (32, 53) Our study design uses this concept of reverse pharmacology to analyze the behavior of known inhibitors on several species of CFTR rather than in mutagenesis studies. The benefit of using cross species analysis is that we avoid the limitations of mutagenesis studies, wherein single amino acid changes disrupt channel function through global changes in the secondary or tertiary structure of the protein.

We studied the effects of three inhibitors on four isoforms of CFTR, each with varying sequence identity to the human isoform and each with distinct sequence motifs. The pharmacologic profiles of each CFTR isoform would be expected to elucidate structure and functional relationships.

Charged Vestibule Model of CFTR

The "charged vestibule model", described by Green and Andersen in 1991, proposed that the general features of channel structure are the result of evolutionary pressure due to the limitations on the rate of ion conduction imposed by diffusion. (16) They reviewed theoretical and experimental data, which suggested that the

rapid ion translocation across the thickness of a biological membrane could only be possible if the narrow region of the pore responsible for selectivity and binding, is flanked by vestibules designed to increase the capture radius at the channel mouth, and to concentrate permeable ions by electrostatic means. (21) This model is widely used in the literature (17, 54) to explain structure-function relationships of CFTR.

Figure 9: *The charged vestibule model of CFTR mediated chloride transport.* Site directed mutagenesis studies have implicated several positively charged amino acids in the vestibules and pore in the attraction and binding of chloride. (17, 21, 22, 28, 55-56) Experimental studies suggest that GlyH-101 occludes the pore extra-cellularly and that glibenclamide occludes chloride transport intra-cellularly. (31, 40) CFTRinh-172 may act on the R domain to inhibit chloride conductance. (36-39)

The charged vestibule model proposes that the CFTR channel pore consists of three regions: an outer vestibule, pointing towards the outside of the cell

membrane, a narrow region, which is the rate limiting area of the selectivity filter and an inner vestibule, that is opened towards the cytoplasm. (Figure 9)

Because CFTR is predominantly permeant to negatively charged chloride ions, positive charges within the pore are theorized to promote the accumulation of chloride and to create a conditioned environment adjacent to the rate-limiting narrow section of the pore. Several site-specific mutagenesis experiments have observed changes in conductance and current-voltage rectification secondary to mutations made within the CFTR pore. These observations suggested that positively single charged residues are an essential part of the outer and inner vestibules. Several permeant anion binding sites exist. The positive charges in the outer vestibule are R334 and K335 in TM6 and R104 and R117 in extracellular loop 1 and the positive charges in the inner vestibule are K95 and R303 in TM1 and TM5. (17, 28, 55-56) These amino acids are considered important in drawing extracellular and intracellular chloride anions respectively into the central narrow pore region. The residues R347 and R352, both present in TM6 are a part of the R domain but are theorized to be important in permeation, open state stability and structural integrity. The residues, F337, T338 and S341 are present in the narrow region of the pore and may play role in the rate limiting steps of anion permeation. (21-22) As CFTR specific inhibitors GlyH101 and Glibenclamide are both

negatively charged and the CFTRinh-172 is at least hydrophobic, these positively charged amino acids important in chloride anion attraction and binding may also be important binding sites for inhibition by small molecules. (40, 35) The negatively charged inhibitors may therefore be competing with chloride anions for affinity and binding within the CFTR pore providing a mechanism for occlusion and inhibition. (Figure 10)

CFTRinh-172: sCFTR and residues 347 and R352

We demonstrated in three experimental models, including, (1) two electrode voltage clamping (TEVC) of *Xenopus laevis* oocytes, (2) short circuit current studies in shark rectal gland tissue monolayers from primary tissue culture and (3) intact shark rectal gland perfusions that sCFTR shows nearly no response to CFTRinh-172. TEVC studies further demonstrated that pig and kfCFTR are significantly less responsive to CFTRinh-172 than hCFTR. Recent work provides evidence that CFTRinh-172 interacts directly with CFTR's R domain at a region that is important to formation of the channel. (37) Mutations introduced at R347 and R352 in TM6, replaced arginine with alanine, and demonstrated decreased inhibitory potency in functional assays. (37)

Because of the observation that CFTRinh-172 has decreased potency of inhibition in functional studies with pig and kfCFTR and almost no potency with

sCFTR, we proposed that the amino acids identities at position 347 and 352 were substituted with different amino acids, perhaps not neutral or less positively charged than arginine. However, examination of the sequence alignment of these four CFTR isoforms reveals positions R347 and R352 have perfect consensus. (Figure 10) This sequence conservation suggests that these two residues alone are not sufficient to explain the mechanism of action of CFTRinh-172. Looking closer at the amino acid sequence adjacent to R347 and 352, positions 349 and 356 and 357, were less conserved across species. In human and pig, the non-polar amino acid, alanine, are present at positions 349 and 357 and the polar residue tryptophan is present at position 357. In shark and killifish, these non-polar and polar residues are replaced with threonine and serine respectively, both with partial negative charges. These partial negative charges may decrease the potency of CFTRinh-172 by decreasing the affinity of the polar organic compound to the adjacent positively charged arginine residues. However, this does not explain the observed decreased potency of the inhibitor on pCFTR as the residues in this region are completely conserved with its human isoform.

Glibenclamide: pCFTR and residues K95 and R303

The most striking difference in pharmacologic profiles demonstrated by TEVC studies was that pCFTR mediated chloride conductance was completely

unresponsive to glibenclamide and that kfCFTR showed decreased response when compared to shark and hCFTR. This observation confirmed previously published short circuit current studies that pig was unresponsive to inhibition by glibenclamide. (48) Glibenclamide is thought to block the CFTR channel in a complex mechanism by interacting with multiple binding sites with varying degrees of affinity that is both voltage and pH dependent. Patch clamp studies suggest that glibenclamide blocks CFTR by interacting with two sites within the channel pore and one site that lies in the inner vestibule. (32) The amino acids K95 and R303 have been proposed to be important with glibenclamide's interaction with the inner vestibule. (34, 56) Therefore, we hypothesized that there may exist a species-specific difference in the amino acid sequence at K95 and R303 that accounts for the differences in pharamacologic profiles observed in our TEVC studies. However, examination of the amino acid sequence alignment of the four isoforms demonstrates conservation of these residues suggesting that these residues are not solely responsible for the interactions of glibenclamide with the channel pore. We again examined the amino acid sequence alignment adjacent to K95 and R303. In human and sCFTR the non-polar residues alanine and leucine occupy position 96 and 102. These positions in the killifish isoform are occupied by threonine and serine respectively, which have partial negative charges. This could, again, theoretically explain the differences in inhibitory profile observed with kfCFTR.

However, the residues K95 and R303 are conserved in pCFTR. The absent inhibition of pCFTR mediated conductance may be due to differences in sequence homology between the CFTR isoforms at the two other suggested sites that glibenclamide is theorized to interact with in the channel pore.

GlyH101: Residues R334, K335, R104 and R117

All four CFTR isoforms were rapidly and significantly responsive to GlyH-101 mediated inhibition of chloride conductance. Furthermore, shark and pCFTR were comparatively more responsive to GlyH-101 inhibition than human and kfCFTR, which is in contrast to shark and pCFTRs relative decreased sensitivity to CFTRinh-172 and glibenclamide. GlyH-101 is like glibenclamide, an open channel blocker, but GlyH-101 is unique because it acts by a novel external pore occluding mechanism. Compared with both CFTRinh-172 and glibenclamide, GlyH-101 is >50 fold more water-soluble and is rapid and reversible suggesting it acts at the extracellular face of the channel. The positively charged residues R334, K335, R104 and R117 have been proposed to be essential to GlyH-101's interaction with the outer vestibule. (28, 40, 57) These four residues are conserved in all four species of CFTR studied. As all four isoforms of CFTR are sensitive to GlyH-101 inhibition, the conservation of these four residues may confirm their importance in GlyH-101 function. Examination of the amino acid sequences adjacent to the

positively charged arginine and lysine residues reveals that at position 115 in hCFTR, a strongly negatively charged glutamic acid residue resides, where as in shark and pig CFTR, position 115 is occupied by the neutral residue alanine. Shark CFTR furthermore has a positively charged residue at position 113 which is not present in the other isoforms. Shark CFTR demonstrated rapid inhibition by GlyH-101 even at the smallest concentrations studied. The replacement of a negatively charged residue with a neutral residue, and the addition of a positively charged residue, at region thought to be important for the attraction and binding of the negatively charged GlyH-101 may explain the potency of this particular inhibitor when interacting with shark CFTR.

Figure 10: *Amino Acid Sequence Alignment of Human, Pig, Shark and Killifish CFTR:* Conserved residues that are suggested to be important for CFTR specific inhibitor binding are in bold. Green amino acids are proposed binding sites for CFTRinh 172, red are for glybenclamide, and yellow for glyH-101. The sequence alignment was made using ClustalW2 Alignment and Biological Workbench. Key: "*" means that the residues in the column are identical in all sequences in the alignment. ":" means that conserved substitutions have been observed. "." means that semi-conserved substitutions are observed.

```
Human           MQRSPLEKASVVSKLFFSWTRPILRKGYRQRLELSDIYQIPSVDSADNLSEKLEREWDRE 60
Killifish       MQKSPVEDANFLSRFVFWWITPLLRKGFTKKLELTDVYKAPSFDLADTLSERLEREWDKE 60
Pig             MQRSPLEKASIFSKLFFSWTRPILRKGYRQRLELSDIYHISSSDSADNLSEKLEREWDRE 60
Shark           MQRSPIEKANAFSKLFFRWPRPILKKGYRQKLELSDIYQIPSSDSADELSEMLEREWDRE 60
                **:**:*.*. .*::.* *  *:*:**: ::***:*:*: .* * ** *** ******:*

Human           LAS-KKNPKLINALRRCFFWRFMFYGIFLYLGEVTKAVQPLLLGRIIASYDPDNKEERSI 119
Killifish       VVLAKGRPKLLKALARCFFLPFAFFGVLLYLGEASKTVQPQLSGRIIASFDPFHAAERSQ 120
Pig             LAS-KKNPKLINALRRCFFWRFMFYGIILYLGEVTKAVQPLLLGRIIASYDPDNKAERSI 119
Shark           LATSKKNPKLVNALRRCFFWRFLFYGILLYFVEFTKAVQPLCLGRIIASYNAKNTYEREI 120
                :.  * .***::** ****  * *:*::**: * :*:***   ******::. :  **.

Human           AIYLGIGLCLLFIVRTLLLHPAIFGLHHIGMQMRIAMFSLIYKKTLKLSSRVLDKISIGQ 179
```

```
Killifish       GYYLALGLGLLFTARFILLQPAIYGLHHLGMQIRIALFSLIYKKTLKLSSKVLDKISTGQ 180
Pig             AIYLGVGLCLLFIVRTLLLHPAIFGPHHIGMQMRIAMFSLIYKKTLKLSSRVLDKISIGQ 179
Shark           AYYLALGLCLLFVVRTLFLHPAVFGLQHLGMQMRIALFSLIYKKILKMSSRVLDKIDTGQ 180
                . **.:** *** .* ::*:**::* :*:***:***:******* **:**:*****. **

Human           LVSLLSNNLNKFDEGLALAHFVWIAPLQVALLMGLIWELLQASAFCGLGFLIVLALFQAG 239
Killifish       LVSLMSAHLNKLDESLGLAHFVWITPLQCILCTGLIWELIEVNGFCALASLTLLGILQAW 240
Pig             LVSLLSNNLNKFDEGLALAHFVWIAPLQVTLLMGLLWELLQASAFCGLAFLVVLALFQAG 239
Shark           LVSLLSNNLNKFDEGVAVAHFVWIAPVQVVLLMGLIWNELTEFVFCGLGFLIMLALFQAW 240
                ****:* :***:**.:.:******:*:*  *  **:*: :    **.*. * :*.::**

Human           LGRMMMKYRDQRAGKISERLVITSEMIENIQSVKAYCWEEAMEKMIENLRQTELKLTRKA 299
Killifish       LSLKMGPPRAQRAGLINRRLALTSEIVENIHSVKAYGWEEVMETIIKNIRQDEMTLTRKI 300
Pig             LGKMMMKYRDQRAGKINERLVITSEMIENIQSVKAYCWEEAMEKMIENLRQTELKLTRKA 299
Shark           LGKKMMQYRDKRAGKINERLAITSEIIDNIQSVKVYCWEDAMEKIIDDIRQVELKLTRKV 300
                *.  *   * :*** *..**.:***:::**:***.* **:.**.:*.::** *:.****

Human           AYVRYFNSSAFFFSGFFVVFLSVLPYALIKGIILRKIFTTISFCIVLRMAVTRQFPWAVQ 359
Killifish       GSLRYFYSASYFFSAILVIVSAIVPHALSNGIILRRIFTTASYCVVLRMTLTRQLPGSIQ 360
Pig             AYVRYFNSSAFFFSGLFVVFLSVLPYALLKGIMLRKIFTTISFCIVLRMAVTRQFPWAVQ 359
Shark           AYCRYFSSSAFFFSGFFVVFLSVVPYAFIHTIKLRRIFTTISYNIVLRMTVTRQFPSAIQ 360
                .  *** *:::***.::*:. :::*:*: : * **:**** *: :****::***:* ::*
```

Modulation of Channel Gating

The unique interactions observed between the GlyH-101, CFTRinh-172 and glibenclamide and different species of CFTR despite amino acid sequence conservation in the charged vestibule and regulatory domains may also be explained by the complex nature of species specific channel kinetics and by the binding affinity or equilibrium dissociation constant of each inhibitor. The macroscopic conductance G_j for ion j is given by:

$$G_j = g_j \times N \times P_o$$

where is g_j the individual conductance of each channel, N is the number of available channels in a given membrane and P_o is open probability of that channel. In our studies, we assumed that the number of available channels measured during each experiment did not affect the percent inhibition of maximal stimulation. We furthermore, assumed that channel conductance, g_j, did not differ between species of CFTR and that the open probability of each channel were similar and that small differences did not contribute to the macroscopic conductance measured. However, identical $G_j = g_j \times N \times P_o$, do not necessarily imply identical g_j, N or P_o: for example a small number of channels with a greater open probability may be equal to a large number of channels with a low open probability. Several recent studies have revealed single channel conductance differences between *xenopus laevis*, human and shark CFTR: *xenopus laevis* CFTR demonstrates significantly greater g_j than the human and shark isoforms. Furthermore single channel conductance studies demonstrate differences between the open probabilities of CFTR isoforms. A notably reduced P_o of mouse CFTR was observed when compared with rodent (59, 60) and human CFTR (61). The gating behavior of mouse CFTR has also been observed to be dramatically different than human CFTR with differing patterns of channel openings and closures. (61, 62) Glibenclamide, GlyH-101 and CFTRinh-

172 are all open channel inhibitors (63, 40, 64) that act by presumably shortening the open time but not the closed time of the channel. The rate of association and disassociation of these inhibitors with their binding sites may be influenced by the kinetics of opening and closing of each channel. Therefore, the individual channel kinetic characteristics and the binding affinities of each inhibitor may influence the macroscopic differences in conduction and inhibition observed.

Conclusion: Questioning the Single Amino Acid Binding Models.

In summary, we demonstrate in this study and confirm previously reported observations (41, 40, 48) that cross species examination of the CFTR protein reveals unique pharmacologic profiles for several CFTR specific inhibitors. These distinct species differences cannot be explained by reverse pharmacology because the proposed amino acids that these inhibitors interact with are uniformly conserved across the species studied and thus cannot account for the differences in function observed. This study suggests that the binding of the inhibitors with the channel vestibule and pore is likely the result of a complex interaction involving multiple amino acids at multiple sites. Ion transport is dependent on the unique matrix of charged residues in the vestibules and pore, which create electrostatic potentials that increase conductance by increasing the concentration of chloride. In this complex picture of selectivity, the positioning of positively or partially charged residues is

vital to channel function.

Therefore, the differences in inhibition demonstrated across diverse CFTR species cannot be explained by simply targeting one amino acid for site-directed mutagenesis. Rather, the potency of inhibitory actions of CFTRinh-172, GlyH-101 and gibenclamide on the CFTR molecule is dictated by the local environment and the three dimensional structure of residues that form the vestibule and the chloride pore and regulatory domain. The identity of the amino acids that play important roles in binding and inhibition may not fully be understood until the crystal structure of the CFTR protein is solved.

References

1. Sheppard DN & Welsh MJ (1999) Structure and function of the CFTR chloride channel. Physiol Rev 79(1 Suppl):S23-45.
2. Kidd JF, Kogan I, & Bear CE (2004) Molecular basis for the chloride channel activity of cystic fibrosis transmembrane conductance regulator and the consequences of disease-causing mutations. Curr Top Dev Biol 60:215-249.
3. Davis PB, Drumm M, Konstan MW. Cystic fibrosis. *Am J Respir Crit Care Med*. Nov 1996;154(5):1229-56.
4. Bobadilla,J.L.; Macek,M.,Jr; Fine,J.P.; Farrell,P.M. (2002) Cystic fibrosis: a worldwide analysis of CFTR mutations--correlation with incidence data and application to screening. Hum. Mutat,19 (6): 575-606
5. Rowe,S.M.; Miller,S.; Sorscher,E.J. (2005) Cystic Fibrosis. New England Journal of Medicine 352 (19)
6. Gibson RL; Burns JL; Ramsey BW (2003) Pathophysiology and management of pulmonary infections in cystic fibrosis. Am J Respir Crit Care Med 168(8): 918-51.
7. Collins FS (1992) Cystic fibrosis: molecular biology and therapeutic implications.Science. 256(5058): 774-9.
8. Denning GM; Ostedgaard LS; Cheng SH; Smith AE; Welsh MJ (1992) Localization of cystic fibrosis transmembrane conductance regulator in chloride secretory epithelia. J Clin Invest. (1):339-49.
9. Pilewski JM & Frizzell RA (1999) Role of CFTR in airway disease. Physiol Rev 79(1 Suppl):S215-255.
10. Dean M, Rzhetsky A, & Allikmets R (2001) The human ATP-binding cassette (ABC) transporter superfamily. Genome Res 11(7):1156-1166.
11. Akabas MH (2000) Cystic fibrosis transmembrane conductance regulator. Structure and function of an epithelial chloride channel. J Biol Chem 275(6):3729-3732.
12. Vergani P, Lockless SW, Nairn AC, & Gadsby DC (2005) CFTR channel opening by ATP-driven tight dimerization of its nucleotide-binding domains. Nature 433(7028):876-880.
13. Buchwald M, Tsui LC, & Riordan JR (1989) The search for the cystic fibrosis gene. Am J Physiol 257(2 Pt 1):L47-52.
14. Riordan JR, et al. (1989) Identification of the cystic fibrosis gene: cloning and characterization of complementary DNA. Science 245(4922):1066-1073.

15. Rosenberg MF, Kamis AB, Aleksandrov LA, Ford RC, & Riordan JR (2004) Purification and crystallization of the cystic fibrosis transmembrane conductance regulator (CFTR). J Biol Chem 279(37):39051-39057 .
16. Green WN & Andersen OS (1991) Surface charges and ion channel function. Annu Rev Physiol 53:341-359.
17. Smith SS, et al. (2001) CFTR: covalent and noncovalent modification suggests a role for fixed charges in anion conduction. J Gen Physiol 118(4):407-431 .
18. Moorhouse AJ, Keramidas A, Zaykin A, Schofield PR, & Barry PH (2002) Single channel analysis of conductance and rectification in cation-selective, mutant glycine receptor channels. J Gen Physiol 119(5):411-425).
19. Tabcharani JA, et al. (1993) Multi-ion pore behaviour in the CFTR chloride channel. Nature 366(6450):79-82.
20. Mansoura MK, et al. (1998) Cystic fibrosis transmembrane conductance regulator (CFTR) anion binding as a probe of the pore. Biophys J 74(3):1320-1332.
21. Smith SS, Steinle ED, Meyerhoff ME, & Dawson DC (1999) Cystic fibrosis transmembrane conductance regulator. Physical basis for lyotropic anion selectivity patterns. J Gen Physiol 114(6):799-818.
22. Dawson DC, Smith SS, & Mansoura MK (1999) CFTR: mechanism of anion conduction. Physiol Rev 79(1 Suppl):S47-75.
23. Linsdell P (2001) Relationship between anion binding and anion permeability revealed by mutagenesis within the cystic fibrosis transmembrane conductance regulator chloride channel pore. J Physiol 531(Pt 1):51-66.
24. Gong X & Linsdell P (2003) Coupled movement of permeant and blocking ions in the CFTR chloride channel pore. J Physiol 549(Pt 2):375-385.
25. Gong X & Linsdell P (2003) Mutation-induced blocker permeability and multiion block of the CFTR chloride channel pore. J Gen Physiol 122(6):673-687.
26. Gong X & Linsdell P (2004) Maximization of the rate of chloride conduction in the CFTR channel pore by ion-ion interactions. Arch Biochem Biophys 426(1):78-82.
27. Ge N, Muise CN, Gong X, & Linsdell P (2004) Direct comparison of the functional roles played by different transmembrane regions in the cystic fibrosis transmembrane conductance regulator chloride channel pore. J Biol Chem 279(53):55283-55289.

28. Gong X & Linsdell P (2003) Molecular determinants and role of an anion binding site in the external mouth of the CFTR chloride channel pore. J Physiol 549(Pt 2):387-397.
29. Tabcharani JA, Linsdell P, & Hanrahan JW (1997) Halide permeation in wild-type and mutant cystic fibrosis transmembrane conductance regulator chloride channels. J Gen Physiol 110(4):341-354.
30. McDonough S, Davidson N, Lester HA, & McCarty NA (1994) Novel pore-lining residues in CFTR that govern permeation and open-channel block. Neuron 13(3):623-634.
31. Zhou Z, Hu S, & Hwang TC (2002) Probing an open CFTR pore with organic anion blockers. J Gen Physiol 120(5):647-662.
32. Schultz BD, Singh AK, Devor DC, & Bridges RJ (1999) Pharmacology of CFTR chloride channel activity. Physiol Rev 79(1 Suppl):S109-144.
33. Cai Z, Lansdell KA, & Sheppard DN (1999) Inhibition of heterologously expressed cystic fibrosis transmembrane conductance regulator Cl- channels by non-sulphonylurea hypoglycaemic agents. Br J Pharmacol 128(1):108-118.
34. Sheppard DN & Robinson KA (1997) Mechanism of glibenclamide inhibition of cystic fibrosis transmembrane conductance regulator Cl-channels expressed in a murine cell line. J Physiol 503 (Pt 2):333-346.
35. Zhang ZR, Zeltwanger S, & McCarty NA (2004) Steady-state interactions of glibenclamide with CFTR: evidence for multiple sites in the pore. J Membr Biol 199(1):15-28.
36. Ma T, et al. (2002) Thiazolidinone CFTR inhibitor identified by high-throughput screening blocks cholera toxin-induced intestinal fluid secretion. J Clin Invest 110(11):1651-1658.
37. Caci E, et al. (2008) Evidence for direct CFTR inhibition by CFTR(inh)-172 based on Arg347 mutagenesis. Biochem J 413(1):135-142.
38. Thiagarajah JR, Broadbent T, Hsieh E, & Verkman AS (2004) Prevention of toxin-induced intestinal ion and fluid secretion by a small-molecule CFTR inhibitor. Gastroenterology 126(2):511-519.
39. Thiagarajah JR, Song Y, Haggie PM, & Verkman AS (2004) A small molecule CFTR inhibitor produces cystic fibrosis-like submucosal gland fluid secretions in normal airways. FASEB J 18(7):875-877.
40. Muanprasat C, et al. (2004) Discovery of glycine hydrazide pore-occluding CFTR inhibitors: mechanism, structure-activity analysis, and in vivo efficacy. J Gen Physiol 124(2):125-137.
41. Ratner MA, Decker SE, Aller SG, Weber G, & Forrest JN, Jr. (2006) Mercury toxicity in the shark (Squalus acanthias) rectal gland: apical CFTR

chloride channels are inhibited by mercuric chloride. J Exp Zool A Comp Exp Biol 305(3):259-267.

42. Weber GJ, et al. (2006) Mercury and zinc differentially inhibit shark and human CFTR orthologues: involvement of shark cysteine 102. Am J Physiol Cell Physiol 290(3):C793-801.
43. Gong X, Burbridge SM, Lewis AC, Wong PY, & Linsdell P (2002) Mechanism of lonidamine inhibition of the CFTR chloride channel. Br J Pharmacol 137(6):928-936.
44. Zhang ZR, Zeltwanger S, & McCarty NA (2000) Direct comparison of NPPB and DPC as probes of CFTR expressed in Xenopus oocytes. Membr Biol 175(1):35-52.
45. Walsh KB, Long KJ, & Shen X (1999) Structural and ionic determinants of 5-nitro-2-(3-phenylprophyl-amino)-benzoic acid block of the CFTR chloride channel. Br J Pharmacol 127(2):369-376.
46. Gupta J & Linsdell P (2002) Point mutations in the pore region directly or indirectly affect glibenclamide block of the CFTR chloride channel. Pflugers Arch 443(5-6):739-747.
47. Ostedgaard LS, et al. (2007) Processing and function of CFTR-DeltaF508 are species-dependent. Proc Natl Acad Sci U S A 104(39):15370-15375.
48. Liu X, et al. (2007) Bioelectric properties of chloride channels in human, pig, ferret, and mouse airway epithelia. Am J Respir Cell Mol Biol 36(3):313-323.
49. Bewley, M., Decker, S., Klein, C., Ratner, M., Kelley, C., Burks, K., Motley, W., Peters, A., Forrest, J.N. The CFTR inhibitor-172 has minimal effects on shark CFTR as compared to human CFTR. Bull. Mt Desert Isl. Biol. Lab, 43, 28-29.
50. Bewley,M.S.; Pena,J.T.; Plesch,F.N.; Decker,S.E.; Weber,G.J.; Forrest,J.N.,Jr (2006) Shark rectal gland vasoactive intestinal peptide receptor: cloning, functional expression, and regulation of CFTR chloride channels. Am.J.Physiol.Regul.Integr.Comp.Physiol., 291 (4) R1157-6443.
51. Valentich JD & Forrest JN, Jr. (1991) Cl- secretion by cultured shark rectal gland cells. I. Transepithelial transport. Am J Physiol 260(4 Pt 1):C813-823.
52. Silva P, Epstein FH, Karnaky KJ, Jr., Reichlin S, & Forrest JN, Jr. (1993) Neuropeptide Y inhibits chloride secretion in the shark rectal gland. Am J Physiol 265(2 Pt 2):R439-446.
53. McCarty NA (2000) Permeation through the CFTR chloride channel. J Exp Biol 203(Pt 13):1947-1962.

54. Sheppard DN (2004) CFTR channel pharmacology: novel pore blockers identified by high-throughput screening. J Gen Physiol 124(2):109-113.
55. Aubin CN & Linsdell P (2006) Positive charges at the intracellular mouth of the pore regulate anion conduction in the CFTR chloride channel. J Gen Physiol 128(5):535-545.
56. Linsdell P (2005) Location of a common inhibitor binding site in the cytoplasmic vestibule of the cystic fibrosis transmembrane conductance regulator chloride channel pore. J Biol Chem 280(10):8945-8950.
57. Zhou JJ, Fatehi M, & Linsdell P (2008) Identification of positive charges situated at the outer mouth of the CFTR chloride channel pore. Pflugers Arch 457(2):351-360.
58. Lester, H.A. (1991) Strategies for studying permeation at voltage- gated ion channels. Annu. Rev. Physiol. 53:477–496.
59. Gray M A, Greenwell J R, Argent B E. (1988) Secretin-regulated chloride channel on the apical plasma membrane of pancreatic duct cells. Journal of Membrane Biology. 105:131–142
60. French P J, van Doorninck J H, Peters R H P C, Verbeek E, Ameen N A, Marino C R, De Jonge H R, Bijman J, Scholte B J. (1996) A ΔF508 mutation in mouse cystic fibrosis transmembrane conductance regulator results in a temperature-sensitive processing defect in vivo. Journal of Clinical Investigation. 98:1304–1312.
61. Lansdell KA, Delaney SK, Lunn DP, Thomson SA, Sheppard DN, Wainwright BJ (1998) Comparison of the gating behavior of human and murine cystic fibrosis transmembrane conductance regulator Cl- channels expressed in mammalian cells. Journal of Physiology 508 (2): 379-392
62. Winter M C, Sheppard D N, Carson M R, Welsh M J. (1994) Effect of ATP concentration on CFTR Cl^- channels: a kinetic analysis of channel regulation. Biophysical Journal. 66:1398–1403.
63. Shultz BD, DeRoos, ADG, Venglarik CJ, Singh AK, Frizell RA, Bridges RJ. (1996) Glibenclamide blockade of CFTR chloride channels. 271 (2): 192
64. Kopeikin Z, Li M, Hwang TC (2009) On the Mechanism of CFTR inhibition by CFTRinh-172. Biophysical Journal. 96(3): 469a